



Theoretical and numerical study of highly anisotropic turbulent flows

L. Biferale^{a,d,*}, I. Daumont^a, A. Lanotte^{b,d}, F. Toschi^{c,d}

^a *Dipartimento di Fisica, Università “Tor Vergata”, Via della Ricerca Scientifica 1, 00133, Roma, Italy*

^b *CNR, ISAC – Sezione di Lecce, Str. Prov. Lecce-Monteroni Km 1.200, 73100, Lecce, Italy*

^c *CNR, Istituto per le Applicazioni del Calcolo, Viale del Policlinico 137, 00161, Roma, Italy*

^d *INFN, Unità di Tor Vergata, Via della Ricerca Scientifica 1, 00133, Roma, Italy*

Received 10 February 2003; received in revised form 12 June 2003; accepted 30 October 2003

Abstract

We present a detailed numerical study of *anisotropic* statistical fluctuations in stationary, *homogeneous* turbulent flows. We address both problems of intermittency in anisotropic sectors, and the relative importance of isotropic and anisotropic fluctuations at different scales on a direct numerical simulation of a three-dimensional *random* Kolmogorov flow.

We review a simple argument to predict the dimensional scaling for all velocity moments, in all anisotropic sectors. We extend a previous analysis made on the same data set (Phys. Rev. Lett. 86 (2001) 4831) presenting (i) the statistical behavior of spectra and co-spectra; (ii) high-order longitudinal structure functions; (iii) anisotropic fluctuations of the full tensorial two-points velocity correlations. Among the many issues discussed, we stress the problem of the *return-to-isotropy*, the universality of anisotropic fluctuations and the foliation mechanism. A new *a priori* test on sub-grid quantities used in Large-Eddy Simulations is also presented.

© 2003 Elsevier SAS. All rights reserved.

Keywords: Turbulence; Anisotropy; Intermittency; LES

1. Introduction

Kolmogorov 1941 theory assumes local homogeneity and local isotropy: the memory of large scale anisotropic forcing and/or boundary conditions is supposed to be lost during the process of energy transfer toward small scales. The overall result is a local recovery of isotropy and of universality in the statistics of turbulent fluctuations at scales small enough and at high Reynolds numbers. In recent years, a quantitative investigation of return-to-isotropy in experimental anisotropic turbulence [2–6], numerical homogeneous shear flows [7,8] and numerical channel flows [9], questioned the main Kolmogorov paradigm, speaking explicitly of *persistence of anisotropies*. A huge amount of theoretical work has been done, starting from [10], in order to understand how to link the rotational invariance of Navier–Stokes equations with the properties of anisotropic velocity correlations. Quantifying anisotropic effects in small scale turbulence is both a *theoretical* challenge and a very actual *practical* problem, opening the question whether any realistic turbulent flow can ever possess statistical features independent of the – generally anisotropic – boundary and forcing effects. Neglected anisotropic effects have also been proposed to be at the origin of different statistical properties of transversal and longitudinal velocity fluctuations [11]. The importance of properly disentangling isotropic and anisotropic fluctuations has been demonstrated in the analysis of intermittency in channel flow turbulence [12]. Investigating and developing proper small scales models for anisotropic turbulence is also a first-order

* Corresponding author.

E-mail address: Luca.Biferale@roma2.infn.it (L. Biferale).

question appearing in all Large-Eddy Simulations (LES) of turbulent flows close to rigid walls or affected by anisotropic body forces [13].

Important steps forward in the analysis of anisotropic fluctuations have recently been made in the context of Kraichnan models [14–16], i.e., passive scalars/vectors advected by isotropic, Gaussian and white-in-time velocity fields with large-scale anisotropic forcing [17–21]. In those models, anomalous scaling for the isotropic and anisotropic fluctuations of the passive fields arises as the result of a non-trivial structure of the advecting operator. First, scaling exponents are found to be universal: they do not depend on the actual value of forcing and boundary conditions. Second, they are fully characterized by the order of the anisotropy: correlation functions in different sectors of the rotational group in 3 dimensions, $SO(3)$, show different scaling properties. Non-universal effects are felt only in coefficients multiplying the power laws, when imposing the matching with non-universal boundary conditions at large scales. Similar questions, like the existence of scaling laws in the anisotropic sectors, or the values of the scaling exponents and their universal character, are at the forefront of experimental, numerical and theoretical research of real turbulent flows. Notwithstanding the diffuse interest in the problem, only quite recently indirect experimental investigations of scaling in different sectors [22,3,6] and direct decomposition in numerical simulations [12,23,9] have been attempted.

The situation is still under debate: evidences of a clear improving of scaling laws by isolating the isotropic sector have been reported, supporting the idea that the undecomposed correlations are strongly affected by the superposition of isotropic and anisotropic fluctuations [12]. Experimental evidences of the existence of a scaling law also in anisotropic sectors have been reported [22,3,6]. The value of the anisotropic leading exponent for the second order correlation function is found to be close to the dimensional estimate $\xi_2^{\text{ani}} = 4/3$ [24]. Most of the experimental investigations are flawed by the contemporary presence of anisotropies and strong non-homogeneities; in some specific cases the meaning of scaling can however be re-interpreted (see for instance [25–27] for a detailed analysis of strongly non-homogeneous and/or shear-dominated flows).

This paper is intended to give a comprehensive exposition of some recent numerical results concerning the statistics of the velocity field, when energy is injected into the system via a strong anisotropic *homogeneous* forcing, confined to large scales [1]. We performed numerical investigations of a 3D random Kolmogorov flow (RKF): the resulting velocity field was strongly anisotropic but statistically homogeneous. For the RKF, previous analyses have been reported in [1,28]. Here, we present a more extended study, by providing further information on anisotropies in both real and Fourier spaces. We present a first systematic attempt to validate one of the most popular LES model on the basis of its performances on purely anisotropic correlation functions. We also present direct measurements of isotropic and anisotropic sectors of even and odd structure functions, up to the sixth order. We review in detail a dimensional prediction able to extend Lumley's argument for any moment of the velocity field and for any kind of anisotropic fluctuation [28]. All results point toward the existence of anisotropic universal anomalous scaling, i.e., anisotropic structure functions possess scaling exponents which deviate from their dimensional estimate. We present a first attempt to exactly decompose all tensorial components of the second order velocity correlation, $\langle v_i(\mathbf{x} + \mathbf{r})v_j(\mathbf{x}) \rangle$, into their isotropic and anisotropic components and we discuss the puzzle of the – supposed – different scaling between longitudinal and transversal isotropic correlation functions [29,30,5].

The paper is organized as follows. In Section 2, we briefly review the dynamical importance of rotational invariance for the Navier–Stokes equations and its consequences on the *foliation* of the correlation function hierarchy [10]. In Section 3 we present the numerical measurements for isotropic and anisotropic fluctuations in both real and Fourier spaces for the RKF, as well as a consistent dimensional argument for the scaling of any anisotropic fluctuations. We also discuss how to assess the return to isotropy in a quantitative way using the decomposition in the irreducible representations of the group of rotations in 3 dimensions, $SO(3)$. We present the first $SO(3)$ decomposition of the full tensorial structure of two-point velocity correlations. Section 4 is devoted to some *a priori* tests of a popular LES model, the so-called nonlinear model, on the database of the random Kolmogorov flow.

2. $SO(3)$ invariance and foliation of correlation hierarchy

In this section, we review recent results focusing on the dynamical and statistical consequences of invariance under rotation of the advective term of the Navier–Stokes equations. In particular, we discuss how the above property allows one to introduce a systematic tool able to quantify in an exact way the degree of anisotropy at each scale. The typical questions addressed are (i) how to quantify the tendency toward isotropy in hydro-dynamical problems, (ii) how to measure persistence of anisotropies (if any), (iii) how to quantify the robustness (read universality) of anisotropic fluctuations at small scales.

The above issues have a number of theoretical and applied interests. In many realistic turbulent problems where anisotropy enters in the game, it is relevant to disentangle universal from non-universal aspects, as well as leading from sub-leading scaling behaviors. The starting point is the observation that the Navier–Stokes equations, neglecting the non-universal boundary conditions and the external forcing, are invariant under spatial rotations. A natural way to understand the inertial range statistical properties is to suppose that both boundary conditions and forcing give a dominant contribution only at large scales, while the

transfer of fluctuations from large to small scales in the bulk is driven by the inertial – rotational invariant – terms. This is the rationale to study velocity correlation functions in terms of the projection on the irreducible representations of the SO(3) group.

Let us fix the idea by writing the Navier–Stokes equation for the two-points homogeneous structure function: $S^{\alpha\beta}(\mathbf{r}) \equiv \langle (v_\alpha(\mathbf{r}) - v_\alpha(0))(v_\beta(\mathbf{r}) - v_\beta(0)) \rangle$. It is simple to derive the equation for this observable:

$$\partial_t S^{\alpha\beta}(\mathbf{r}) = -\partial_\mu S^{\alpha\beta\mu}(\mathbf{r}) + \partial^\beta P^\alpha(\mathbf{r}) + \nu \partial^2 S^{\alpha\beta}(\mathbf{r}) - F^{\alpha\beta}(\mathbf{r}), \quad (1)$$

where we have introduced, with obvious notation, the third order structure function $S^{\alpha\beta\mu}(\mathbf{r})$; the velocity–pressure correlation function, $P^\beta(\mathbf{r}) \equiv \langle (p(\mathbf{r}) - p(-\mathbf{r}))v_\beta(0) \rangle$ and the forcing-velocity correlation function, $F^{\alpha\beta}(\mathbf{r}) \equiv \langle f_\alpha(\mathbf{r})v_\beta(0) + f_\alpha(0)v_\beta(\mathbf{r}) \rangle + (\alpha \Leftrightarrow \beta)$. In Eq. (1), only the forcing term $F^{\alpha\beta}(\mathbf{r})$, and the boundary conditions may break the rotational invariance. Both of them are large scale quantities, and we may safely imagine that for scales smaller than the integral scale L_0 , Eq. (1) recovers full rotational invariance in the bulk, with forcing induced terms appearing only as subdominant contributions.

Then, we can project the rotational invariant part of (1) on the irreducible representations of the SO(3) group and obtain a set of dynamical equations for each projection, in each separate sector [10]. More explicitly, let us recall that the decomposition of $S^{\alpha\beta}(\mathbf{r})$ in terms of the *eigenfunction* of the rotational operator is made by a set of functions labelled with the usual indices $j = 0, 1, \dots$ and $m = -j, \dots, +j$, corresponding to the total angular momentum and to the projection of the total angular momentum in an arbitrary direction, respectively. For scalars, as for example the longitudinal structure function, $S_2(\mathbf{r}) \equiv \langle [(\mathbf{v}(\mathbf{r}) - \mathbf{v}(0)) \cdot \hat{\mathbf{r}}]^2 \rangle$, the (j, m) set of basis functions are the spherical harmonics, $Y_{jm}(\hat{\mathbf{r}})$. For a generic p -th order tensor, another index q is necessary, to label different irreducible representations for each j sector [10].

It is easy to show that there are only $q = 1, \dots, 6$ irreducible representations of the SO(3) group for the space of two-indices symmetric tensors, as it is $S^{\alpha\beta}(\mathbf{r})$ (see Appendix). The second order structure function can be exactly decomposed as:

$$S^{\alpha\beta}(\mathbf{r}) \equiv \sum_{q=1}^6 \sum_{j=0}^{\infty} \sum_{m=-j}^{+j} S_{qjm}^{(2)}(r) B_{qjm}^{\alpha\beta}(\hat{\mathbf{r}}), \quad (2)$$

where the $B_{qjm}^{\alpha\beta}(\hat{\mathbf{r}})$ are tensors defined on the unit sphere which can be seen as a generalization of the spherical harmonics to the tensorial case. The superscript “2” in the coefficient of (2) reflects the order of the analyzed correlation function. The importance of decomposition (2) stems from the fact that one can exactly disentangle, for each anisotropic projection, the statistical dependency on the reference scale, r .

The physics of isotropic and anisotropic fluctuations can now be analyzed in a systematic and quantitative way by studying the projection coefficients $S_{qjm}^{(2)}(r)$. It is important to realize that these obey separate dynamical equations within each (j, m) sector. Indeed by applying the same decomposition to all correlations (except for the forcing) appearing in (1), and noticing that all derivative operators are rotational invariant, we obtain the *foliation* of the dynamical equation for any correlation, in each given sector (j, m) of the rotational group. Only projections within the same (j, m) sector are coupled [10]. The *foliation* is a consequence of the fact that the unforced Navier–Stokes equations contain only rotationally invariant operators and of the *linearity* of the correlation function hierarchy. Moreover, in the limit of infinite Reynolds numbers, the Navier–Stokes equations become scaling invariant, sector by sector. It is quite natural to expect the existence of scaling laws characterizing each sector separately:

$$S_{qjm}^{(2)}(r) \sim c_{qjm}^{(2)} r^{\xi_j^{(2)}}, \quad (3)$$

where the coefficients $c_{qjm}^{(2)}$ are fixed by imposing the matching with the large-scale physics. This result can be exactly demonstrated in models for passive advection of scalars and vectors [18,20,21], but can only be argued for the Navier–Stokes case on the basis of the above mentioned properties of rotational invariance of the operators, and linearity of the hierarchy. The foliation of the scaling behavior has of course two important consequences. First, the undecomposed observable is built up with contributions (isotropic and anisotropic) having different scaling laws, i.e., the undecomposed, raw correlations do not scale:

$$S^{\alpha\beta}(\mathbf{r}) \sim \sum_{q=1}^6 [c_{q00}^{(2)} r^{\xi_0^{(2)}} B_{q00}^{\alpha\beta}(\hat{\mathbf{r}}) + c_{q10}^{(2)} r^{\xi_1^{(2)}} B_{q10}^{\alpha\beta}(\hat{\mathbf{r}}) + \dots]. \quad (4)$$

Decomposition similar to (2) can be written for the most general p -th order tensor, $S^{\alpha_1 \dots \alpha_p}(\mathbf{r}) \equiv \langle (v_{\alpha_1}(\mathbf{r}) - v_{\alpha_1}(0)) \dots (v_{\alpha_p}(\mathbf{r}) - v_{\alpha_p}(0)) \rangle$ made of p velocity differences at separation \mathbf{r} :

$$S^{\alpha_1 \dots \alpha_p}(\mathbf{r}) \sim \sum_q \sum_{jm} S_{qjm}^{(p)}(r) B_{qjm}^{\alpha_1 \dots \alpha_p}(\hat{\mathbf{r}}). \quad (5)$$

Scaling is recovered either looking at the contributions in separate sectors, $S_{qjm}^{(p)}(r) \sim r^{\xi^j(p)}$, or looking at scales small enough such that only the leading term in the sum (5) dominates.

This is connected to the important question of *recovering of isotropy*. Such a recovering may exist only if the isotropic scaling exponent is always smaller than all anisotropic ones for any given order p of the decomposed correlation function: $\xi^{j=0}(p) < \xi^j(p)$ for all j . Moreover, a hierarchy among the different anisotropic exponents is naturally expected, *within* any given order p :

$$\xi^{j=0}(p) \leq \xi^{j=1}(p) \leq \xi^{j=2}(p) < \dots \quad (6)$$

Another important consequence of (5) is that undecomposed objects are strongly *non-universal*, because the coefficients $c_{qjm}^{(p)}$, giving the overall strength of each sector depend obviously on the large-scale set-up. Only scaling exponents $\xi^j(p)$ may be assumed to enjoy some robustness properties. In addition, scaling exponents are supposed to be independent of the (m, q) indices. For the Navier–Stokes problem, there are no rigorous statements: again, hints come from analytical results derived in the class of linear models previously mentioned. In particular, the independence from the m index is given by the arbitrariness in defining the orientation of the reference axis in 3D space.

The dependence/independence from the q index, i.e., from the set of irreducible representations used to decompose the observables in each (j, m) sector, is on the other hand much less trivial and has interesting consequences. A dependence on the q index would weaken the whole *foliation* mechanism, which is based on the idea that only properties invariant under rotations are relevant for the inertial range statistics, and not the set of eigenfunctions (with the same rotational properties) chosen to decompose the observables. For example, the only possible way to support, theoretically, the observed different scaling between transversal and longitudinal high-order structure functions in isotropic statistics [29,30,5] would be to admit that, in the isotropic sector, projections with different q -indices have different scaling properties. This sounds quite unlikely. A much simpler scenario is to imagine that the observed differences are due to spurious contaminations from sub-leading anisotropic sectors not completely decayed, yet: that is, such differences would become smaller and smaller by going to larger and larger Reynolds numbers.

In the following we first review a simple argument to predict the *dimensional* values of scaling exponents, of any order p and for any sector j . Then, we present a detailed analysis of the numerical data set issuing from the numerical simulation of a homogeneous random Kolmogorov flow with resolution 256^3 . In particular, we discuss the measurements of scaling exponents in (j, m) sector up to $j = 6$, for structure functions up to the sixth order. This enables us to assess (i) the existence of a hierarchical organization of scaling exponents (6); (ii) to establish in a quantitative way the rate of recovery of isotropy, and (iii) to support the statement that anisotropic fluctuations are anomalous, i.e., do not follow the dimensional prediction made in Section 3.1. Finally, in Section 3.5 we discuss the q dependency of the SO(3) decomposition by performing the whole decomposition of the second rank tensor $S^{\alpha\beta}(\mathbf{r})$ up to $j = 2$. In the latter case, we also consider the problem of longitudinal vs. transversal scaling.

3. Anisotropic scaling

3.1. A dimensional estimate for the scaling in the $j \neq 0$ sectors

To give an assessment of the normal or anomalous behavior of anisotropic fluctuations, we first need an estimate for the dimensional values of the exponents $\xi^j(p)$. In [28], a new dimensional argument for the scaling exponents of the structure functions of any order, and any sector was introduced. The argument is based on the idea that large-scale energy pumping and/or boundary conditions are such as to enforce a large-scale anisotropic driving velocity field \mathbf{U} . A prediction for intermediate (small) scale anisotropic fluctuations may then be obtained by studying the influence of the large-scale \mathbf{U} on the inertial range. By decomposing the velocity field, $\mathbf{v} = \mathbf{u} + \mathbf{U}$, in a small scale component \mathbf{u} , and a large-scale anisotropic component \mathbf{U} , we have the following equation for \mathbf{u} :

$$\partial_t u_\alpha + u_\beta \partial_\beta u_\alpha + U_\beta \partial_\beta u_\alpha + u_\beta \partial_\beta U_\alpha = -\partial_\alpha p + \nu \Delta u_\alpha. \quad (7)$$

The major effect of the large-scale field is given by the instantaneous shear, $\partial_\beta U_\alpha$, which acts as an anisotropic forcing term on small scales.

A matching argument can be built as follows. Let us first consider the equation of motion for two point quantities $\langle u_\delta(\mathbf{x}') u_\alpha(\mathbf{x}) \rangle$ in the stationary regime. We may balance inertial and shear-induced contributions:

$$\langle u_\delta(\mathbf{x}') u_\beta(\mathbf{x}) \partial_\beta u_\alpha(\mathbf{x}) \rangle \sim \langle \partial_\mu U_\alpha(\mathbf{x}) u_\delta(\mathbf{x}') u_\mu(\mathbf{x}) \rangle, \quad (8)$$

which allows for a dimensional estimate of the anisotropic components of the LHS, in terms of the RHS shear intensity and of the $\langle uu \rangle$ isotropic part. Similarly for three point quantities we have (neglecting tensorial notation): $\langle uuu \partial u \rangle \sim \langle \partial U uuu \rangle$, which

can be generalized to any order velocity correlation. The shear term is a large-scale “slow” quantity and therefore, as far as scaling properties are concerned, we may safely estimate: $\langle \partial_\mu U_\alpha(\mathbf{x}) u_\delta(\mathbf{x}') u_\mu(\mathbf{x}) \rangle \sim \Sigma_{\alpha\mu} \langle u_\delta(\mathbf{x}') u_\mu(\mathbf{x}) \rangle$.

The 3×3 matrix $\Sigma_{\alpha\beta}$ is associated to the combined probability to have a given shear and a given small scale velocity configuration. The $\Sigma_{\alpha\beta}$ tensor brings angular momentum only up to $j = 2$. One may therefore argue, by using simple composition of angular momenta, ($j = 2 \otimes j = 2$), the following dimensional matching:

$$\mathcal{S}_j^{(p)}(r) \sim r |\Sigma| \cdot \mathcal{S}_{j-2}^{(p-1)}(r). \quad (9)$$

Here $\mathcal{S}_j^{(p)}(r)$ is a shorthand notation, neglecting further possible dependencies on q and m indices, for the projection on the j -th sector of the p -th order correlation function $S_{qjm}^{(p)}(r)$ introduced in the previous section. In (9) with $|\Sigma|$ we denote the typical intensity of the shear term $\Sigma_{\alpha\beta}$ in the $j = 2$ sector. Due to the simple level of the reasoning, we cannot make any detailed statement about possible dependencies on the q and m indices. We limit to discuss, therefore, the connections between different j sectors.

For instance, the leading behavior of the $j = 2$ anisotropic sector of the 3rd order correlation function in the LHS of (9), is given by the coupling between the $j = 2$ components of $\Sigma_{\alpha\beta}$, and the $j = 0$ sector of the 2nd order velocity correlation in the RHS of (9): $\mathcal{S}_{j=2}^{(3)}(r) \sim r |\Sigma| \mathcal{S}_{j=0}^{(2)}(r) \sim r \xi_d^2(3)$. By using the same argument and considering that now we know the scaling of the sectors $j = 0, 2$ of the third order correlation, we may estimate the scaling exponents of the fourth order correlation for $j = 2, 4$. The procedure is easily extended to all orders, leading to the following expression:

$$\xi_d^j(p) = \frac{p+j}{3}, \quad (10)$$

which has been obtained by neglecting the intermittency effects in the isotropic sector. Let us notice that expression (10) coincides with Lumley prediction [24], done for $p = 2$ and $j = 2$, i.e., it generalizes Lumley’s argument to any kind of anisotropic fluctuations and any order of velocity correlation functions. Let us also notice that prediction (10) differ from the one made in [31], where for simplicity the tensorial properties of all velocity and forcing correlations functions were neglected.

3.2. Validation of numerical simulations

We performed a direct numerical simulation of a 3D fully periodic, incompressible flow with anisotropic large-scale energy injection. The analytic expression of the forcing is $\mathbf{f} = (0, 0, f_z(x))$, with $f_z(x) = F_1 \cos[2\pi x/L_x + \phi_1(t)] + F_2 \cos[4\pi x/L_x + \phi_2(t)]$, with constant amplitudes $F_{\{1,2\}}$ and independent, uniformly distributed, δ -correlated in time random phases $\phi_{\{1,2\}}(t)$. The random phases lead to homogeneous statistics. We studied the RKF at resolution 256^3 , and collected up to 70 eddy turn over times. Such long averaging is necessary because, as in any strongly anisotropic flow, we observe the formation of persistent large-scale structures inducing strong oscillations of the mean energy evolution. The viscous term was replaced by a second-order hyper-viscosity, $-\nu \Delta^2 \mathbf{v}$. Time-marching used a (second-order) slaved Adams–Bashforth scheme. Typical Reynolds number is $Re_\lambda \sim 100$. We have a high degree of homogeneity (deviations are less than 5%) in the two transverse directions, \hat{y} and \hat{z} , while we observe small oscillations in the \hat{x} direction (of the order of 10%); these are due to statistical fluctuations and are averaged out in the limit of very large statistics. In other words we have at each time a Kolmogorov Flow, non-homogeneous in the \hat{x} direction, which tends to get more and more homogeneous thanks to the random-reshuffling of forcing phases.

In Fig. 1 we plot the instantaneous energy spectrum, $E(k) = \int_{|\mathbf{k}'|=k} \langle \mathbf{v}(\mathbf{k}') \cdot \mathbf{v}^*(\mathbf{k}') \rangle d\mathbf{k}'$. It exhibits a scaling very close to the K41 isotropic behavior $\propto k^{-5/3}$. Also, purely anisotropic quantities such as the co-spectra, $E_{\alpha\beta}(k_\mu) = \int \langle v_\alpha(\mathbf{k}) \cdot v_\beta^*(\mathbf{k}) \rangle dk_\delta dk_\gamma$, with $(\delta, \gamma) \neq \mu$ show a good agreement with the $k^{-7/3}$ law predicted by Lumley in [24]. These results validate our numerical simulation: they are in agreement with common observations in numerical simulations [32], and in experiments [4], in the presence of different anisotropic large-scale forcings.

3.3. SO(3) analysis of longitudinal structure functions

Let us now discuss the SO(3) decomposition of longitudinal structure functions: $S^{(p)}(\mathbf{r}) = \langle [(\mathbf{v}(\mathbf{x} + \mathbf{r}) - \mathbf{v}(\mathbf{x})) \cdot \hat{\mathbf{r}}]^p \rangle$. For scalar objects like the longitudinal structure functions, the SO(3) decomposition reduces to the projection on the spherical harmonics:

$$S^{(p)}(\mathbf{r}) = \sum_{j=0}^{\infty} \sum_{m=-j}^j \mathcal{S}_{jm}^{(p)}(r) Y_{jm}(\hat{\mathbf{r}}). \quad (11)$$

As customary, the indices (j, m) label the total angular momentum and its projection on a reference axis, respectively. Our interest here is on the scaling behavior of the functions $S_{jm}^{(p)}(r)$, i.e., $S_{jm}^{(p)}(r) \sim c_{jm} r^{\xi_j^{(p)}}$. We start by reporting in the inset of Fig. 1, some already published results [1] for the isotropic sector. We compare the undecomposed structure functions in the three axis directions, with the projection $S_{00}^{(p)}(r)$. Only for the projected correlation is it possible to measure (with 5% of accuracy) the scaling exponent by a direct log–log fit versus the scale separation. The best fit gives $\xi^{j=0}(2) = 0.70 \pm 0.03$. On the contrary, the undecomposed structure functions are overwhelmed by the anisotropic effects present at all scales, and the scaling behavior is completely spoiled.

In Table 1 we summarize our quantitative findings. Let us stress the accuracy of these results: already at moderate Reynolds numbers, it is possible to detect quite good isotropic scaling laws if anisotropic fluctuations are disentangled correctly. In Fig. 2, there is an overview of the second order structure function for all sectors, isotropic and anisotropic, which have a signal-to-noise ratio high enough to ensure stable results. Sectors with odd j s are absent due to the parity symmetry of the longitudinal structure function. We notice from Fig. 2 a clear foliation in terms of the j index: sectors with the same j but different m s behave very similarly. In Table 1 we present a more quantitative analysis by showing the results of the best power law fits for structure functions of orders $p = 2, 4, 6$. First, we notice the presence of a hierarchical organization as assumed in (6), i.e., there is no saturation for the exponents as a function of the j value. Second, the measured exponents in the sectors $j = 4$ and $j = 6$ are anomalous, i.e., they differ from the dimensional estimate given in the previous section, $\xi_d^j(p) = (j + p)/3$.

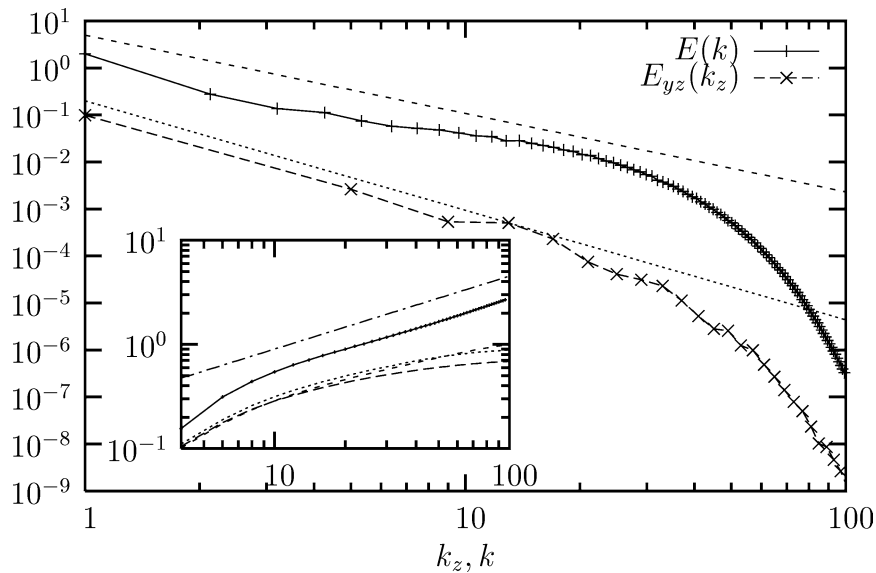


Fig. 1. Log–log plot of instantaneous energy spectrum in the isotropic sector $E(k)$ (top). The straight line is the reference isotropic $k^{-5/3}$ power law. Instantaneous co-spectrum $E_{yz}(k_z)$ (bottom). Here the straight line gives the reference $k_z^{-7/3}$ anisotropic Lumley prediction. The two spectra have been shifted along the vertical direction for the sake of presentation. Inset: analysis on the real space. Log–log plot of $S_{00}^{(2)}(r)$ versus r (top curve), and of the three undecomposed longitudinal structure functions in the three directions x, y, z (three bottom curves). The straight line gives the best fit slope $\xi^{j=0}(2) = 0.7$.

Table 1

We summarize our numerical findings for the scaling exponents in the isotropic and anisotropic sectors. Notice that values for the anisotropic sector $j = 2$ are taken from the experiments [3,6]. For the values extracted from the numerical simulation (columns $j = 0, 4, 6$), error bars are estimated on the oscillation of the local slopes. For the experimental data the error is given as the mismatch between the two experiments. For all sectors we also give the dimensional estimate $\xi_d^j(p) = (p + j)/3$

p	$\xi^{j=0}(p) - \xi_d^{j=0}(p)$	$\xi^{j=2}(p) - \xi_d^{j=2}(p)$	$\xi^{j=4}(p) - \xi_d^{j=4}(p)$	$\xi^{j=6}(p) - \xi_d^{j=6}(p)$
2	0.70 (2) – 0.66	1.15 (5) – 1.33	1.65 (5) – 2.00	3.2 (2) – 2.66
4	1.28 (4) – 1.33	1.56 (5) – 2.00	2.25 (10) – 2.66	3.1 (2) – 3.33
6	1.81 (6) – 2.00	2.07 (8) – 2.33	2.60 (10) – 3.33	3.3 (2) – 4.00

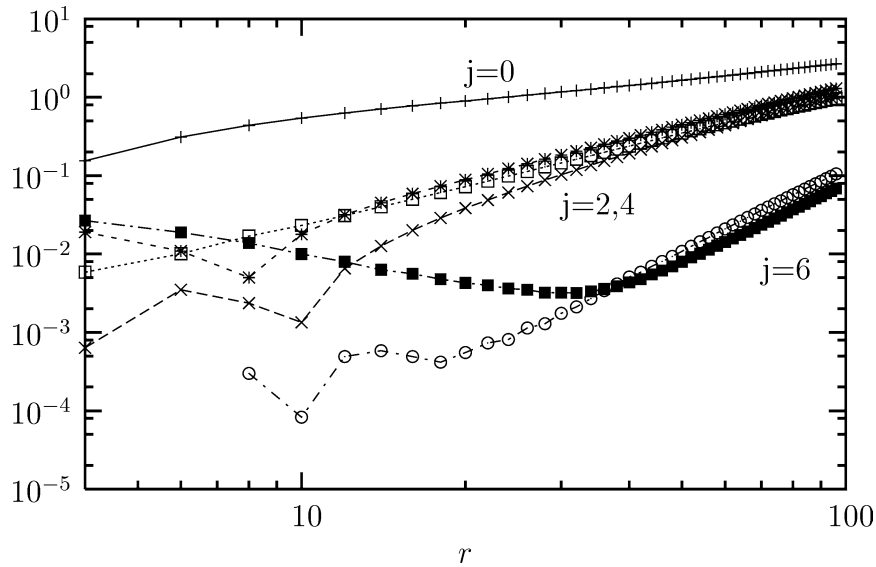


Fig. 2. Log–log plot of the second order structure function in all sectors with a strong signal. Sectors: (0, 0), (+); (2, 2), (×); (4, 0), (□); (4, 2), (★); (6, 0), (○); (6, 2), (■). The statistical and numerical noise induced by the SO(3) projection is estimated as the threshold where the $j = 6$ sector starts to deviate from the monotonic decreasing behavior, i.e., $\mathcal{O}(10^{-3})$.

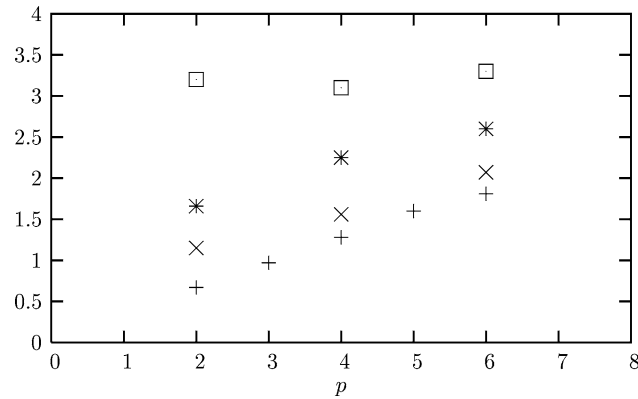


Fig. 3. Scaling exponents, $\xi^j(p)$, of structure functions of order $p = 2, 4, 6$ for isotropic and anisotropic sectors. From the DNS of RKF we have: isotropic sector, $j = 0$ (+); anisotropic sectors, $j = 4$ (★) and $j = 6$ (□). From the experimental data [3,6], we have $j = 2$ (×). For an estimate of error bars see Table 1.

Unfortunately, we are unable to give clean measurements of the $j = 2$ sector. This is because we always observe a change of sign in the projections $S_{2m}^{(p)}(r)$ for any m (and any order p), probably due to some bottleneck effects at scales of the order of the Kolmogorov scale. Such a change of sign does not allow us to have a scaling range extended enough to measure exponents with reasonable accuracy. Still we may check the overall consistency of the foliation and hierarchical organization of scaling exponents by borrowing the scaling exponents in the $j = 2$ sector from two recent experiments [3,6]. In Fig. 3 we inserted, together with our data, the experimental values as extracted from [3,6]. The resulting picture is fully coherent: experimental data coming from the $j = 2$ sector fit well in the global trend. As clear from Table 1, all anisotropic sectors show *anomalous* scaling laws. The presence of anomalous scaling may also be interpreted as a universality property of small-scale anisotropic statistics. Indeed a direct influence of forcing properties on the small-scale velocity fluctuations would always give a trivial scaling [33].

3.4. Return to isotropy

Having defined the meaning of dimensional scaling of anisotropic fluctuations, we discuss the return-to-isotropy issue. Numerical and experimental evidences of persistence of small-scale anisotropic fluctuations have been reported in various instances [1,4,8,9]. The question has many important consequences. We may refer to the breaking of the *return-to-isotropy* behavior, with two different meanings [9]. We can speak of a *strong* violation if the hierarchy (6) is not observed, i.e., if one, or more, anisotropic sectors become leading with respect to the isotropic one. In such a case, at scales small enough, anisotropic fluctuations become the dominant contribution in the turbulent statistics. This would definitely break the phenomenology developed since Kolmogorov theory in 1941, leading also to the existence of strong non-universalities. Indeed, while any real flow must have an isotropic component, independently on the large scale set-up, different anisotropic sectors may be switched on/off depending on the particular experiment. A *strong* violation of the *return-to-isotropy* postulate has never been observed in Navier–Stokes turbulence. On the other hand, a *weak* breaking of the *return-to-isotropy* corresponds to the existence of dimensionless observables which are exactly zero in a perfectly isotropic ensemble, but which go to zero at small scales with a rate slower than predicted on the basis of dimensional analysis, or eventually do not decrease at all. For instance, by using the simple SO(3) decomposition of longitudinal structure function one may build up anisotropic indicators as:

$$F_{jm}^{(p)}(r) = \frac{S_{jm}^{(p)}(r)}{(S_{00}^{(2)}(r))^{p/2}} \sim r\chi^j(p) \quad (12)$$

with $\chi^j(p) = \xi^j(p) - \frac{p}{2}\xi^0(2)$. Clearly, observables like (12) must go to zero with a power law $F_{jm}^{(p)}(r) \sim r^{j/3}$, if the dimensional scaling (10) is satisfied. What is observed in both experimental and numerical turbulence is that the decaying behavior is much slower and, in some cases, even absent [4,9]: anisotropic fluctuations normalized by the root mean squared isotropic fluctuations do not decay. This is still in agreement with the hierarchy supposed in (6), where only the relative importance of anisotropic fluctuations with respect to the isotropic one of the *same* correlation function are compared. The breaking of the dimensional recovery-of-isotropy is simply due to the existence of anomalous scaling in the anisotropic sectors. If this is the case, the exponents, $\chi^j(p)$, governing the LHS of (12) can assume values much smaller than the dimensional estimate $\xi^j(p) - \frac{p}{2}\xi^0(2) < j/3$, including the possibility to become negative! In Fig. 4, we present the rate of recovery of isotropy for observables of the kind (12), compared with our dimensional prediction, as measured in the RKF data. Despite the existence of the hierarchy (6) quantified in the Table 1, we have a slower recovery-of-isotropy, due to the anomalous anisotropic scaling, in agreement with the explanation above. Furthermore, let us notice that the experimental measurements made in [6] show a clear tendency for the smallest anisotropic exponent, $\xi^{j=2}(p)$ to become closer and closer to the isotropic exponent, $\xi^{j=0}(p)$, for p high enough ($p \geq 8$). Thus, the hierarchy (6) tends to saturate the inequality between the $j = 0$ and $j = 2$ sectors.

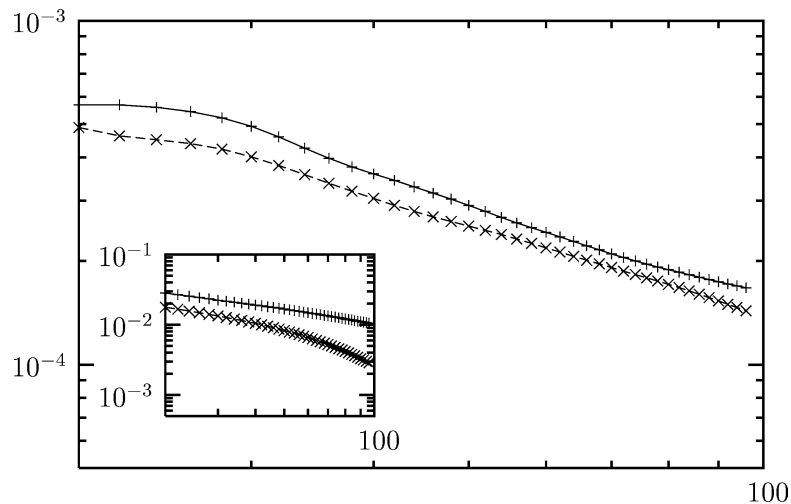


Fig. 4. Persistence of anisotropies. Log–log plot of the dimensionless anisotropic (12) compensated with their dimensional prediction: $F_{jm}^{(p)}(r)/r^{j/3} = (S_{jm}^{(p)}(r)/(S_{00}^{(2)}(r))^{p/2})(1/r^{j/3})$ vs. r . Curves refer to the case $j = 6, m = 0, p = 6$ (+) and $j = 6, m = 0, p = 5$ (x). Inset: the same quantities with $p = 5$ and $p = 6$, but for the anisotropic sector $j = 4$. The observed anisotropic fluctuations are clearly much larger than what is predicted by dimensional analysis.

This is a situation where anisotropic fluctuations are as intense as the isotropic ones: a sort of strong persistence of anisotropies. Unfortunately, the statistics collected in the DNS do not allow us to make a quantitative statement on such high order moments.

3.5. Decomposition of the second rank tensor $S^{\alpha\beta}(\mathbf{r})$

In the previous sections, we have analyzed the scaling properties of scalar quantities built in terms of velocity correlations. For these, the SO(3) projection reduces to the usual decomposition with the spherical harmonics, and does not probe any dependency from the index q labelling different irreducible representations (4). In particular, giving the set of eigenfunctions listed in the Appendix, it is clear that longitudinal structure functions coincide with projections on the $q = 1$ basis tensor. Here we present the first attempt to decompose the whole second-rank tensor, $S^{\alpha\beta}(\mathbf{r})$, for $j = 0, 2$, performing the decomposition (2). In the inset of Fig. 5, there are the only two functions alive in the isotropic sector, $S_{100}^{(2)}(r)$ and $S_{300}^{(2)}(r)$, corresponding to the projection on the tensor $B_{100}^{\alpha\beta}(\hat{\mathbf{r}}) = r^\alpha r^\beta$ (longitudinal) and the projection on the tensor $B_{300}^{\alpha\beta}(\hat{\mathbf{r}}) = (\delta^{\alpha\beta} - r^\alpha r^\beta / r^2)$ (transversal), respectively. In the isotropic sector, the incompressibility constraint forces the two components to have the same scaling. Indeed, as can be seen in the figure, the two scaling behaviors are pretty much the same. Nothing can be said rigorously for the anisotropic sectors. In particular the incompressibility constraint is no more sufficient to force all sectors to have the same scaling (see Appendix of [10]). In the body of Fig. 5, we also show the four components with a nonvanishing projection in the $j = 2, m = 2$ sector, corresponding to $q = 1, 2, 3, 4$ in the list (.21) of Appendix. Three of such curves have a quite good scaling behavior, while one shows a less steep scaling. This result, if confirmed by other measurements, implies a breaking of the foliation mechanism. Nevertheless, let us notice that the overall intensity of the q -projection with a slow decay is much smaller than two out of the other three projections. It is therefore not clear whether such a slow decay for the $j = 2$ sector may ever become important (i.e., dominant) at some scale or not. Other tests at higher Reynolds numbers must be done before making any strict conclusions. It would be very interesting to extend such analysis to higher anisotropic sectors $j > 2$, and higher correlation functions $p > 2$. The computational effort is far from trivial, because very soon in both cases the number of projections on different eigenfunctions to be measured rapidly increases. Let us make here a comment on the claimed experimental observation [29,30,5] that longitudinal and transversal high-order structure functions in *isotropic* turbulence possess a different scaling exponent. If the statistics are really isotropic, and therefore one may exclude contamination from the anisotropic sectors, then the only possibility to have a different scaling between longitudinal, transversal and mixed longitudinal-transversal components would be to admit that already for the isotropic sector $j = 0$, on changing the q representation, the scaling behavior is different. As we mentioned, this is not possible for structure functions of order $p = 2$, because of the incompressibility constraint, but cannot be ruled out for higher order correlators.

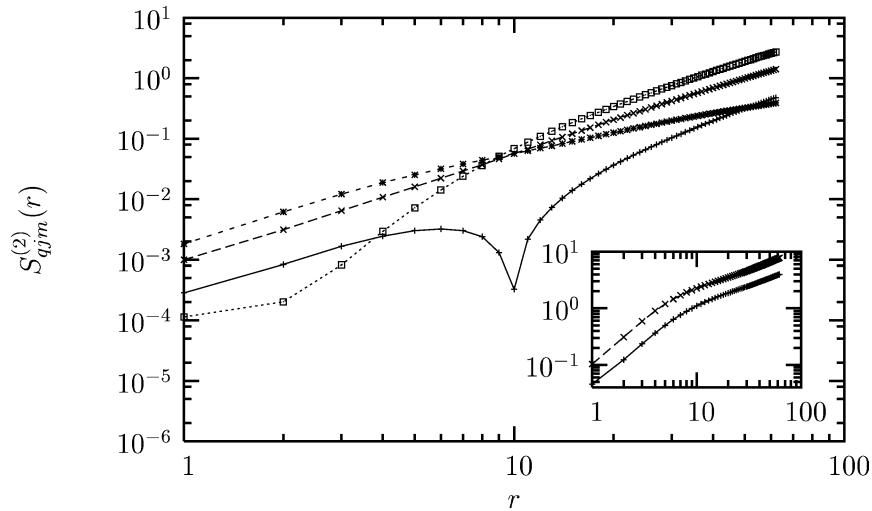


Fig. 5. Log–log plot of the SO(3) decomposition of the second rank tensor, $S^{\alpha\beta}(\mathbf{r})$ vs r . In the inset, we plot the projections on the two isotropic sectors $j = 0$ with $q = 1, 3$, corresponding to the longitudinal $S_{100}^{(2)}(r)$, and transversal structure functions $S_{300}^{(2)}(r)$ (see Appendix for the notation). In the body of the figure, there are the four most intense projections on the anisotropic sectors $S_{qjm}^{(2)}(r)$ with $j = 2, m = 2$: projection $q = 1$ (\square); projection $q = 2$ ($+$); projection $q = 3$ (\star), and projection $q = 4$ (\times). Notice that three out of four have roughly the same scaling, while $q = 3$ has a slower decay. Nevertheless, $q = 3$ is much less intense than $q = 1$ and $q = 4$ for all inertial scales.

4. An application of SO(3) decomposition to Large-Eddy Simulation

The presence of strong large-scale anisotropies makes the RKF an ideal candidate to test small-scale modelizations used in Large-Eddy Simulation. In LES, only the large scales of motion are described in a deterministic way, while small scales are parametrized. In the sequel, we show results of what is known under the name of *a priori* tests: starting from DNS data, we compare the behavior between the modeling of some sub-grid observables, and their real statistical behavior. These are the typical zeroth order tests to be done in order to check a priori the degree of reliability of a LES. The interest in making such tests is that we have a strongly anisotropic data set, i.e., an important benchmark for realistic situations.

To get into details, the principle of LES is to focus on large scales, thanks to a low-pass spatial filtering applied to the velocity field: $\mathbf{v} \Rightarrow \tilde{\mathbf{v}} = \int \phi_\Delta(\mathbf{x} - \mathbf{x}') \mathbf{v}(\mathbf{x}') d\mathbf{x}'$, with $\phi_\Delta(\mathbf{x})$ being the convolution kernel. When doing so, the unforced Navier–Stokes equations for the filtered velocity $\tilde{\mathbf{v}}$, and pressure \tilde{p} , are modified by the appearance of a new term proportional to $\partial_\beta \tau_{\alpha\beta}$, where: $\tau_{\alpha\beta} = \tilde{v}_\alpha \tilde{v}_\beta - \tilde{v}_\alpha \tilde{v}_\beta$, is the so-called sub-grid-scale (SGS) stress tensor. In this way, only scales greater than the filter scale Δ are simulated or “resolved”. To close the LES equations, small scale motion has to be modeled, that is the SGS stress tensor has to be expressed in terms of the resolved field $\tilde{\mathbf{v}}$ only. It is worth noticing that in the equation for the resolved total kinetic energy $\tilde{q}^2 = \tilde{v}_\alpha \tilde{v}_\alpha$, there is a term proportional to the SGS stress and to the resolved strain rate $\tilde{R}_{\alpha\beta}$, i.e., $\sim \tau_{\alpha\beta} \tilde{R}_{\alpha\beta}$, whose sign is not a priori defined. When negative, it represents the *effective* dissipation at scales larger than Δ , due to the friction at the small ones (forward cascade); but when positive, the energy flow being reversed, it acts as a source of energy for the large scales (energy back-scatter).

One of the most popular SGS models, describing both forward and backward sub-grid energy transfer is the so-called nonlinear or tensor eddy-viscosity model, first proposed by Leonard [34], and discussed in great detail for homogeneous, isotropic turbulence in [35,13]:

$$\tau_{\alpha\beta}^{\text{nl}} = c_n \Delta^2 \partial_\delta \tilde{v}_\alpha \partial_\delta \tilde{v}_\beta, \quad (13)$$

where c_n is typically a $\mathcal{O}(1)$ constant. In our *a priori* tests, we always used a Gaussian, isotropic, normalized $\int \phi_\Delta(\mathbf{x}) d\mathbf{x} = 1$, filter of the form:

$$\phi_\Delta(\mathbf{x}) = \left(\frac{10}{\pi \Delta^2} \right)^{3/2} \exp\left(-\frac{10|\mathbf{x}|^2}{\Delta^2}\right).$$

For the characteristic wave number of the filter $k_c \equiv \pi/\Delta$, we choose the values 4, 8, 16 and 32.

We start our comparison between the actual values of $\tau_{\alpha\beta}$ and those of the modeled SGS, with measures of one-point quantities. A crude indicator of the similarities between the modeled SGS and the real quantities is given by the linear correlation coefficient $\rho(a, a^{\text{mod}})$, between an observable a and its modeled equivalent a^{mod} . One of the most studied quantities is the energy flux towards small scales. For the nonlinear model, we observe a very high level of correlation, going from $\rho = 0.88$ in the case of $k_c = 4$, to $\rho = 0.98$ in the case of $k_c = 32$. In terms of one point measures, the model performances are not spoiled by the presence of the anisotropy, since these results are very similar to those obtained in [35] for isotropic turbulence. In the sub-grid model (13) the only free parameter is the c_n constant to be optimized at any chosen cut-off. Here we fixed them such as to have a perfect agreement between the mean sub-grid and the true energy dissipation. Once the only free parameter is fixed, one may probe the performance of the model on the rare events by comparing the probability density function (PDF) of the true $\tau_{\alpha\beta}$ and of that one measured on the sub-grid model $\tau_{\alpha\beta}^{\text{nl}}$. Fig. 6 shows, for different choices of the filter scale $\Delta \sim k_c^{-1}$, the probability density function of the local energy flux, $\Phi = \tilde{R}_{\alpha\beta} \tau_{\alpha\beta}$, as calculated from the DNS data, compared with that of the modeled energy flux, $\Phi^{\text{nl}} = \tilde{R}_{\alpha\beta} \tau_{\alpha\beta}^{\text{nl}}$. Except for $k_c = 4$, that is for a cut-off at very large scale, we observe a good agreement between the distributions. In particular, the agreement is really good when we pick a characteristic wavenumber k_c , well in the inertial range.

In order to assess the performance of the nonlinear model on anisotropic quantities, we decompose the tensor eddy-viscosity into an isotropic part, the trace of τ , and an anisotropic part $\tau_{\alpha\beta} - 1/3 \tau_{\delta\delta} \delta_{\alpha\beta}$. For the six off-diagonal components, we obtain rates of linear correlation of about 0.9. Such a good agreement is also found for the whole probability density function: in Fig. 7 the PDF of a purely anisotropic component, $\tau_{\alpha\beta}$ with $\alpha = y$ and $\beta = z$, is shown for two choices of the wavenumber k_c .

The effects of the anisotropy on sub-grid scale modeling appear more important when we consider two-point measures. A natural indicator is the spatial correlation of the resolved velocity field and the gradient of the SGS stress tensor:

$$C_{\alpha\beta}(\mathbf{r}) = \langle \tilde{v}_\alpha(0) \nabla_\delta \tau_{\beta\delta}(\mathbf{r}) \rangle, \quad (14)$$

where the RHS depends only on the separation r because we are considering a homogeneous flow. Let us notice that the symmetric form, $C_{\alpha\beta}(\mathbf{r}) + C_{\beta\alpha}(-\mathbf{r})$, is the *transport* term of the dynamical equation of the second order tensor $\langle \tilde{v}_\alpha(0) \tilde{v}_\beta(\mathbf{r}) \rangle$. We applied the SO(3) decomposition to the function

$$T_{\alpha\beta}(\mathbf{r}) = 2C_{\alpha\beta}(\mathbf{0}) - C_{\alpha\beta}(\mathbf{r}) - C_{\alpha\beta}(-\mathbf{r}) = \sum_{qjm} T_{qjm}(r) B_{qjm}^{\alpha\beta}(\hat{\mathbf{r}}). \quad (15)$$

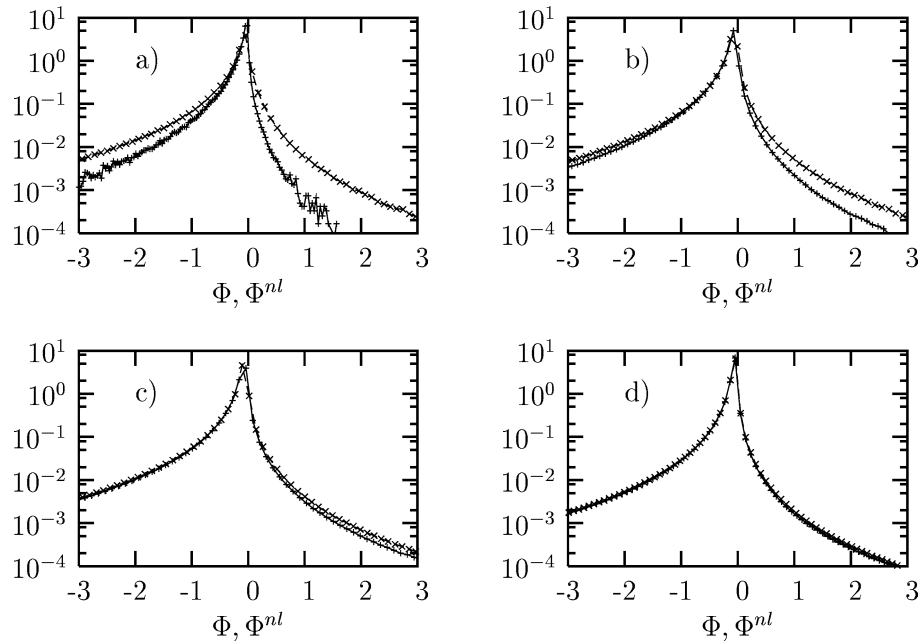


Fig. 6. Log-lin plot of the probability density functions of the true local energy flux $\Phi = \tilde{R}_{\alpha\beta}\tau_{\alpha\beta}$ (+), and the nonlinear model representation $\Phi^{nl} = \tilde{R}_{\alpha\beta}\tau_{\alpha\beta}^{nl}$ (x). The coefficient c_n is fixed in order to enforce the equality of the average flux. Isotropic Gaussian filters are used. Cut-off wavenumber and constants are, respectively: (a) $k_c = 4$, $c_n = 0.049$; (b) $k_c = 8$, $c_n = 0.072$; (c) $k_c = 16$, $c_n = 0.061$; (d) $k_c = 32$, $c_n = 0.056$.

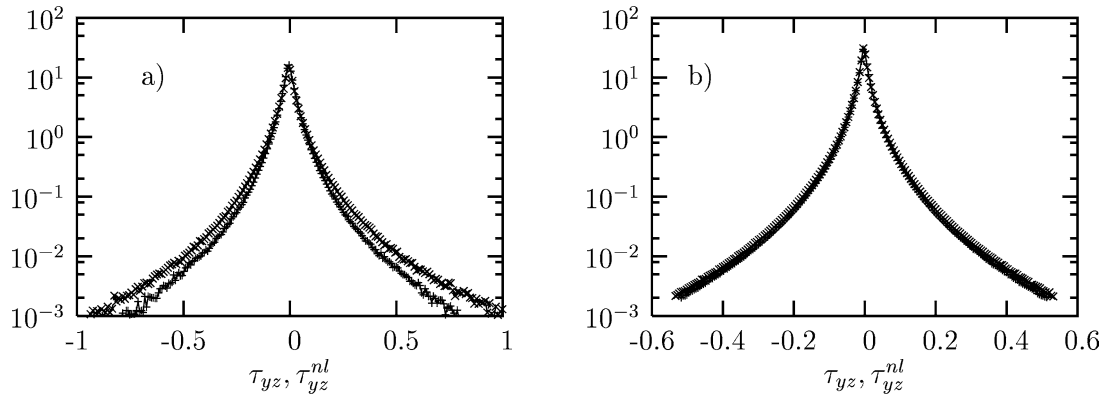


Fig. 7. Probability density functions of the purely anisotropic off-diagonal component τ_{yz} of the SGS stress tensor (+), and of its nonlinear representation τ_{yz}^{nl} (x). Figure (a) $k_c = 8$, $c_n = 0.072$; (b) $k_c = 16$, $c_n = 0.061$. Small discrepancies are observed only for very intense fluctuations in the larger cut-off case (a).

The log-log plot of the isotropic sectors and of some anisotropic ones ($j = 2$, $m = 2$, $q = 2, 4$) are shown in Fig. 8. We note a very good agreement between the isotropic projection coefficient of $T_{\alpha\beta}(r)$, and its nonlinear corresponding $T_{\alpha\beta}^{nl}(r)$. On the other hand, the anisotropic projection coefficients are no longer well fitted by the nonlinear ones, which have a general tendency to overestimate the anisotropy. In other words, as for two point anisotropic fluctuations, the sub-grid model here studied does not perform as well as for the single point quantities once the only free parameter, c_n is fixed by imposing the equality between the sub-grid and the true energy dissipation. To summarize, we can say that even in the presence of a large-scale strong anisotropy, the nonlinear model is able to reproduce the main features of the filtered flow, at least concerning single point measures. Two-point measurements, probing also the correlation of the sub-grid tensor at different spatial locations, perform less well. Still, isotropic two-point measurements are quite well reproduced, while some discrepancies are measured for the most intense anisotropic two-point measurements. It would be extremely interesting to extend this analysis performing a full *a posteriori* test, i.e., undertaking a large-eddy simulation of such a strongly anisotropic flow and comparing the actual performance.

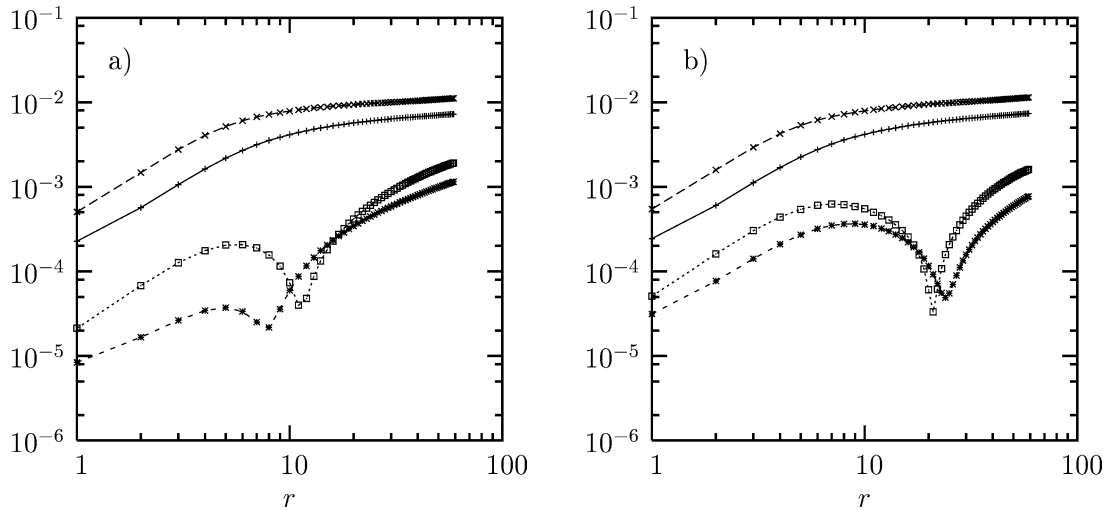


Fig. 8. Log–log plot of the coefficients, $T_{qjm}(r)$, of SO(3) decomposition of the sub-grid correlation (15), at the cut-off $k_c = 16$. (a) True SGS correlation: the two top curves refer to the isotropic sectors $j = 0$ with $q = 1, 3$; while the two bottom curves refer to the most intense projections on the anisotropic sector $j = 2, m = 2$, with $q = 2, 4$. (b) The same as (a), but for the SGS nonlinear model. Notice that the two isotropic projections almost coincide with the true ones showed in panel (a); while there is a clear mismatch in the reproduced intensities and trends for the anisotropic sectors.

5. Conclusions

We presented a detailed numerical study of *anisotropic* statistical fluctuations in stationary, *homogeneous* turbulent flows. We have discussed the meaning of both dimensional and anomalous scaling for the anisotropic turbulent fluctuations. We have extended the numerical results presented in [1], by discussing in detail the recovery of isotropy and the foliation hypothesis. A first detailed measurement of the anisotropic properties of the full tensor second-order velocity correlation was performed. Also, a systematic a priori study of the LES non-linear model in terms of its capability to capture single point and two-point isotropic and anisotropic fluctuations in sub-grid quantities has been performed.

We have given some clear evidences that anisotropic turbulent fluctuations deserve an interest in their own right. They possess the same degree of complexity already well experimented and measured for isotropic fluctuations. They are anomalous, they possess a non-trivial phenomenology and they are much more persistent than what would be believed on the basis of simple dimensional reasonings. Last but not least, they are ubiquitous in any real numerical or experimental turbulent study, including applied problems as for the case of LES. Much more work is needed to extend the available experimental and numerical data base, and to improve experimental techniques enabling one to address in a fully systematic way the SO(3) decomposition on laboratory data. Only after that will simple but basic questions concerning, for example, the degree of universality of anisotropic fluctuations for each SO(3) sector or the *foliation* hypothesis, be answered.

Acknowledgements

We acknowledge useful discussions and collaboration with I. Arad, G. Boffetta, R. Benzi, A. Celani, C. Casciola, B. Jacob, D. Lohse, V. L'vov and I. Procaccia. This research was supported in part by the EU under the Grant No. HPRN-CT 2000-00162 “Non-Ideal Turbulence” and by the INFM (Iniziativa di Calcolo Parallelo). A.L. acknowledges the hospitality of the Observatoire de la Côte d’Azur, where part of this work has been done.

Appendix

We report for completeness the full SO(3) decomposition of the symmetric second order tensor $S^{\alpha\beta}(\mathbf{r})$ [10]. Once fixed j and m indices, the 6 independent basis tensor can be simply constructed starting from the spherical harmonics $Y_{jm}(\hat{\mathbf{r}})$, plus successive application of isotropic operators such as contraction with r_α and $\delta_{\alpha\beta}$, or derivation with respect to ∂_β , saturating the correct number of tensorial indices. A particular choice is the following:

$$B_{1,jm}^{\alpha\beta}(\hat{\mathbf{r}}) \equiv r^{-j-2} r^\alpha r^\beta \Phi_{jm}(\mathbf{r}), \quad (.16)$$

$$B_{2,jm}^{\alpha\beta}(\hat{\mathbf{r}}) \equiv r^{-j} [r^\alpha \partial^\beta + r^\beta \partial^\alpha] \Phi_{jm}(\mathbf{r}), \quad (.17)$$

$$B_{3,jm}^{\alpha\beta}(\hat{\mathbf{r}}) \equiv r^{-j} [\delta^{\alpha\beta} - r^\alpha r^\beta / r^2] \Phi_{jm}(\mathbf{r}), \quad (.18)$$

$$B_{4,jm}^{\alpha\beta}(\hat{\mathbf{r}}) \equiv r^{-j+2} \partial^\alpha \partial^\beta \Phi_{jm}(\mathbf{r}), \quad (.19)$$

$$B_{5,jm}^{\alpha\beta}(\hat{\mathbf{r}}) \equiv r^{-j-1} [r^\alpha \epsilon^{\beta\mu\nu} r_\mu \partial_\nu + r^\beta \epsilon^{\alpha\mu\nu} r_\mu \partial_\nu] \Phi_{jm}(\mathbf{r}), \quad (.20)$$

$$B_{6,jm}^{\alpha\beta}(\hat{\mathbf{r}}) \equiv r^{-j+1} [\epsilon^{\beta\mu\nu} r_\mu \partial_\nu \partial^\alpha + \epsilon^{\alpha\mu\nu} r_\mu \partial_\nu \partial^\beta] \Phi_{jm}(\mathbf{r}), \quad (.21)$$

where $\Phi_{jm}(\mathbf{r}) \equiv r^j Y_{jm}(\hat{\mathbf{r}})$, and $\epsilon^{\alpha\beta\gamma}$ is the usual fully antisymmetric 3-dimensional tensor. The tensors are regrouped according to their parity invariance property: first, those of parity $(-)^j$ (1–4), then those $(-)^{j+1}$ (5, 6).

If the second order tensor under exam did not possess a defined symmetry under the exchange $\alpha \Leftrightarrow \beta$, we would have needed also the following three antisymmetric in addition to the previous six symmetric tensors, to complete the basis:

$$B_{7,jm}^{\alpha\beta}(\hat{\mathbf{r}}) \equiv r^{-j} [r^\alpha \partial^\beta - r^\beta \partial^\alpha] \Phi_{jm}(\mathbf{r}), \quad (.22)$$

$$B_{8,jm}^{\alpha\beta}(\hat{\mathbf{r}}) \equiv r^{-j-1} \epsilon^{\alpha\beta\mu} r_\mu \Phi_{jm}(\mathbf{r}), \quad (.23)$$

$$B_{9,jm}^{\alpha\beta}(\hat{\mathbf{r}}) \equiv r^{-j+1} \epsilon^{\alpha\beta\mu} \partial_\mu \Phi_{jm}(\mathbf{r}). \quad (.24)$$

Clearly, 7 is of parity $(-)^j$ (1–4), and 8, 9 are of parity $(-)^{j+1}$.

References

- [1] L. Biferale, F. Toschi, Anisotropies in homogeneous turbulence: hierarchy of scaling exponents and intermittency of the anisotropic sectors, *Phys. Rev. Lett.* 86 (2001) 4831.
- [2] S. Kurien, V.S. L'vov, I. Procaccia, K.R. Sreenivasan, Scaling structure of the velocity statistics in atmospheric boundary layers, *Phys. Rev. E* 61 (2000) 407.
- [3] S. Kurien, K.R. Sreenivasan, Anisotropic scaling contributions to high-order structure functions in high-Reynolds-number turbulence, *Phys. Rev. E* 62 (2000) 2206.
- [4] X. Shen, Z. Warhaft, The anisotropy of the small scale structure in high Reynolds number ($R_{\lambda} = 1000$) turbulent shear flow, *Phys. Fluids* 12 (2000) 2976.
- [5] X. Shen, Z. Warhaft, Longitudinal and transverse structure functions in sheared and unsheared wind-tunnel turbulence, *Phys. Fluids* 14 (2002) 370.
- [6] Z. Warhaft, X. Shen, On the higher order mixed structure functions in laboratory shear flow, *Phys. Fluids* 14 (2002) 2432.
- [7] A. Pumir, B. Shraiman, Persistent small-scale anisotropy in homogeneous shear flows, *Phys. Rev. Lett.* 75 (1995) 3114.
- [8] A. Pumir, Turbulence in homogeneous shear flows, *Phys. Fluids* 8 (1996) 3112.
- [9] L. Biferale, M. Vergassola, Isotropy vs anisotropy in small-scale turbulence, *Phys. Fluids* 13 (2001) 2139.
- [10] I. Arad, V. L'vov, I. Procaccia, Correlation functions in isotropic and anisotropic turbulence: The role of the symmetry group, *Phys. Rev. E* 59 (1999) 6753.
- [11] B. Dhruva, Y. Tsuji, K.R. Sreenivasan, Transverse structure functions in high-Reynolds-number turbulence, *Phys. Rev. E* 56 (1997) R4928.
- [12] I. Arad, L. Biferale, I. Mazzitelli, I. Procaccia, Disentangling scaling properties in anisotropic and inhomogeneous turbulence, *Phys. Rev. Lett.* 82 (1999) 5040.
- [13] C. Meneveau, J. Katz, Scale-invariance and turbulence models for large-eddy simulation, *Annu. Rev. Fluid Mech.* 32 (2000) 1.
- [14] R.H. Kraichnan, Anomalous scaling of a randomly advected passive scalar, *Phys. Rev. Lett.* 72 (1994) 1016.
- [15] K. Gawędzki, A. Kupiainen, Anomalous scaling of the passive scalar, *Phys. Rev. Lett.* 75 (1995) 3834.
- [16] M. Vergassola, Anomalous scaling for passively advected magnetic fields, *Phys. Rev. E* 53 (1996) R3021.
- [17] A. Lanotte, A. Mazzino, Anisotropic nonperturbative zero modes for passively advected magnetic fields, *Phys. Rev. E* 60 (1999) R3483.
- [18] I. Arad, L. Biferale, I. Procaccia, Nonperturbative spectrum of anomalous scaling exponents in the anisotropic sectors of passively advected magnetic fields, *Phys. Rev. E* 61 (2000) 2654.
- [19] I. Arad, V. L'vov, E. Podivilov, I. Procaccia, Anomalous scaling in the anisotropic sectors of the Kraichnan model of passive scalar advection, *Phys. Rev. E* 62 (2000) 4904.
- [20] N.V. Antonov, J. Honkonen, Anomalous scaling in two models of passive scalar advection: Effects of anisotropy and compressibility, *Phys. Rev. E* 63 (2001) 036302.
- [21] I. Arad, I. Procaccia, Spectrum of anisotropic exponents in hydrodynamic systems with pressure, *Phys. Rev. E* 63 (2001) 056302.
- [22] I. Arad, B. Dhruva, S. Kurien, V.S. L'vov, I. Procaccia, K.R. Sreenivasan, Extraction of anisotropic contributions in turbulent flows, *Phys. Rev. Lett.* 81 (1998) 5330.

- [23] L. Biferale, D. Lohse, I.M. Mazzitelli, F. Toschi, Probing structures in channel flow through $SO(3)$ and $SO(2)$ decomposition, *J. Fluid Mech.* 452 (2002) 39.
- [24] J.L. Lumley, Similarity and the turbulent energy spectrum, *Phys. Fluids* 10 (1967) 855.
- [25] F. Toschi, G. Amati, S. Succi, R. Benzi, R. Piva, Intermittency and structure functions in channel flow turbulence, *Phys. Rev. Lett.* 82 (1999) 5044.
- [26] F. Toschi, E. Levêque, G. Ruiz-Chavarria, Shear effects in nonhomogeneous turbulence, *Phys. Rev. Lett.* 85 (2000) 1436.
- [27] P. Gualtieri, C.M. Casciola, R. Benzi, G. Amati, R. Piva, Scaling laws and intermittency in homogeneous shear flow, *Phys. Fluids* 14 (2002) 583.
- [28] L. Biferale, I. Daumont, A. Lanotte, F. Toschi, Anomalous and Dimensional scaling in anisotropic turbulence, *Phys. Rev. E.* 66 (2002) 056306.
- [29] S. Chen, K.R. Sreenivasan, M. Nelkin, N. Cao, Refined similarity hypothesis for transverse structure functions in fluid turbulence, *Phys. Rev. Lett.* 79 (1997) 2253.
- [30] T. Gotoh, D. Fukayama, T. Nakano, Velocity field statistics in homogeneous steady turbulence obtained using a high-resolution direct numerical simulation, *Phys. Fluids* 14 (2002) 1065.
- [31] S. Grossmann, A. Von der Heydt, D. Lohse, Scaling exponents in weakly anisotropic turbulence from the Navier–Stokes equation, *J. Fluid Mech.* 440 (2001) 381.
- [32] T. Ishihara, K. Yoshida, Y. Kaneda, Anisotropic velocity correlation spectrum at small scales in a homogeneous turbulent shear flow, *Phys. Rev. Lett.* 15 (2002) 154501.
- [33] L. Biferale, G. Boffetta, A. Celani, A. Lanotte, F. Toschi, M. Vergassola, The decay of homogeneous anisotropic turbulence, *Phys. Fluids* 15 (2003) 2105.
- [34] A. Leonard, Energy cascade in large-eddy simulations of turbulent flows, *Adv. Geophys.* 18 (1974) 237.
- [35] V. Borue, S.A. Orszag, Local energy flux and subgrid-scale statistics in three-dimensional turbulence, *J. Fluid Mech.* 366 (1998) 1.